IEEE Open Access Journal of
Power and Energy

Received 4 February 2020; revised 29 March 2020; accepted 19 May 2020. Date of publication 25 May 2020;
date of current version 18 June 2020.

Digital Object Identifier 10.1109/OAJPE.2020.2996949

Fast Frequency Support From Wind Turbine Systems by Arresting Frequency Nadir Close to Settling Frequency

XIANXIAN ZHAO[1,2], YING XUE[1] (Member, IEEE), and XIAO-PING ZHANG[1] (Fellow, IEEE)

[1]Department of Electronic, Electrical and Systems Engineering, University of Birmingham, Birmingham B15 2TT, U.K.
[2]School of Electrical and Electronic Engineering, University College Dublin, Belfield, D04 R7R0 Ireland
CORRESPONDING AUTHOR: XIAO-PING ZHANG (x.p.zhang@bham.ac.uk)

This work was supported in part by EPSRC under Grant EP/N032888/1 and Grant EP/L017725/1.

ABSTRACT The recent power cut incident in the UK on 9th August 2019 indicated that frequency control to raise frequency nadir and eliminate frequency second dip is highly desirable for power grids with high penetration of wind energy. This paper proposes a fast frequency support scheme for wind turbine systems (WTSs) that can enable frequency nadir to be significantly raised and close to the settling frequency and eliminate frequency second dip. In the proposed frequency support scheme, in order to achieve similar frequency support performance and ensure stability of WTSs under varying wind speeds, different levels of wind power penetration and system conditions, an adaptive gain, which is a function of real-time rotor speed and wind power penetration level, is proposed. In the proposed scheme, rotor speeds of WTSs are proposed not to be recovered to the optimal operating points during the primary frequency control, but recovered during the secondary frequency control. Simulation results on the IEEE two-area power system with a doubly fed induction generator (DFIG)-based wind farm and the IEEE 39-bus power system with permanent magnetic synchronous generator (PMSG)-based wind farms using real-time digital simulator (RTDS) and Dymola are presented to verify the effectiveness of the proposed scheme.

INDEX TERMS Wind turbine system, fast frequency support, frequency second dip, frequency nadir, rate of change of frequency (ROCOF), primary frequency control.

NOMENCLATURE

DFIG	Doubly fed induction generator
FN	Frequency nadir
FSD	Frequency second dip
MPPT	Maximum power point tracking
PLL	Phase-locked loop
PMSG	Permanent magnetic synchronous generator
ROCOF	Rate of change of frequency
SG	Synchronous generator
WF	Wind farm
WTS	Wind turbine system
pl	Wind power penetration level
P_m	Mechanical power output of a SG turbine
v_w	Wind speed input to a WTS
K_{opt}	Optimal coefficient for the maximum wind power capture
ω_r	Rotor speed of a DFIG or PMSG
$\omega_{r\mathrm{opt}}$	Optimal rotor speed under MPPT control
$\omega_{r\max}$	Rated rotor speed
$\omega_{r\min}$	Cut-in rotor speed
$\omega_{r\lim}$	Rotor speed threshold below which the proposed frequency support scheme is not allowed
f_{sys}	Grid frequency
f_{nom}	Nominal grid frequency
Δf	Frequency deviation
df/dt	Frequency derivative
$K_p(\omega_r, pl)$	Dynamic gain of Δf in the proposed fast frequency support scheme
$g(pl)$	Dynamic gain in $K_p(\omega_r, pl) = g(pl)k(\omega_r)$ to adapt to different wind power penetration levels
$k(\omega_r)$	Dynamic gain in $K_p(\omega_r, pl) = g(pl)k(\omega_r)$ to adapt to different wind speeds

This work is licensed under a Creative Commons Attribution 4.0 License. For more information, see https://creativecommons.org/licenses/by/4.0/

I. INTRODUCTION

WITH the increasing level of wind power penetration, frequency stability of power system has drawn considerable attentions from system operators [1], [2], as currently the dominant variable speed wind turbine systems (WTSs) are mostly operating at maximum power point tracking (MPPT) mode and thus do not regulate their active power to support the power grid when the grid frequency deviates from its nominal value. Therefore, under the same disturbances, rate of change of frequency (ROCOF) is increased and frequency nadir (FN) becomes lower with higher levels of wind power penetration [3]. A low FN is highly undesirable as it will trigger Low Frequency Demand Disconnection (LFDD) which will cause significant disruptions to electricity consumers. For example, 1 million customers lost their power during the 9th August 2019 event in the UK due to the FN of 48.8 Hz, triggering the automatic LFDD [1]. To address the problem, a number of methods have been proposed, among which exploiting the potential capability of variable speed WTSs to provide inertial and primary frequency response is one of the promising solutions [4], [5], which is more effective for low-inertia power systems.

When the wind speed is higher than the rated value, the additional energy for frequency support by variable speed WTSs can be easily extracted from wind without particular control designs. However, it is challenging when wind speed is below the rated value since WTSs are normally performing MPPT control. When wind speed is below the rated value, potential strategies can be divided into two groups. In the first group, WTSs are operated at a de-loaded condition to have some active power margin that can be used when an increase of generation for inertial or frequency support is needed [3], [6]. Although this strategy leads to a secure power reserve in the system, it causes financial and efficiency losses for wind farm owners. In the second group, WTSs are performing the MPPT control under normal operations and support the grid during a frequency event for a short period of time by releasing the kinetic energy stored in the rotating masses. With this method, no considerable loss of revenue and efficiency will incur during normal operations but the level of support that can be provided is less than that of the first group. This paper focuses on the second group.

In the second group, the methods of frequency support by controlling the rotating kinetic energy can be further divided into two subgroups. In the first subgroup, the rotor speed of a WTS is required to recover to the MPPT (or optimal) operating point after several seconds of over-production of power to support the frequency regulation. As the restoration process requires reduction of output power from WTSs for rotor speed recovery [7]–[9], there is a compromise to be made between the amount of kinetic energy to be released and the recovery speed of rotor speed. This means that if a large amount of kinetic energy is released to support the frequency and the recovery time is short, a big frequency second dip (FSD) will happen. If the released kinetic energy is small for a faster rotor speed recovery, the level of frequency support is limited [10]. In order to avoid big FSD and smoothly restore WTSs to the MPPT operating point, methods [10]–[12] have been proposed to carefully design the over-production and restoration processes. However, the simulation results in [10]–[12] have shown that it took 30 to 70 seconds for rotor speed to be restored to the optimal point after a frequency event. The duration is as long as primary frequency control in many countries. In the second subgroup, the design of the gains for the additional df/dt (rate of change of frequency) or Δf (frequency deviation) loops to adapt different wind speeds and ensure stable operation of WTSs during frequency support is the main focus in these papers [13]–[15], while the issues of rotor speed recovery strategy and the FN being raised to be close to the settling frequency of primary frequency control under high and medium wind speeds have neither been mentioned nor highlighted.

Based on analysis above, this paper presents a fast frequency support scheme to arrest FN to be close to the settling frequency whilst ensuring the stable operation of WTSs under variable wind speeds, different levels of wind power penetration and system conditions. The first target is realized by a new speed recovery strategy that the rotor speeds of WTSs are not restored to MPPT operating points during primary frequency control, but will be automatically recovered during the period of secondary frequency control. As a result, the proposed frequency support scheme releases more kinetic, and it lasts for a longer time than the existing schemes when the rotor speed is restored during primary frequency control, so that FN using the new scheme can be raised to be close to the settling frequency with no concern of FSD.

Another challenge is how to ensure the stability of WTSs and the frequency improvement mentioned above under variable wind speeds, different levels of wind power penetration and system conditions. In the proposed approach, simply adding an extra term, which is the product of Δf and an adaptive gain, can overcome the above challenge. The use of Δf as the feedback signal to support grid frequency simplifies the controller design process, which can adapt to different frequency events and system conditions, and simplifies the process of parameters determination. The proposed adaptive gain, which is a function of real-time rotor speed ω_r and wind power penetration level, can ensure the stability of WTSs by controlling the rotor speed to be above the minimum speed limit, and similar frequency support performance under various wind speeds and different wind power penetration levels.

The main contributions of the proposed frequency support method are summarized as follows:

- FN can be significantly raised to be close to the settling frequency of primary frequency control under both medium and high wind speeds, without FSD. This cannot be achieved with any of the existing methods.

- A new recovery strategy is proposed. No complicated design for rotor speed recovery is required. In this new strategy, the rotor speed will automatically recover with the frequency during secondary frequency control.
- The proposed adaptive gain can significantly achieve the FN improvement not only under different wind speeds but also under different wind power penetration levels. Meanwhile the stability of WTSs in any wind conditions and frequency events can be ensured.
- The proposed adaptive gain vs wind power penetration level can be determined by simulations and can be updated when there are significant changes of operating conditions.
- The proposed control can be easily integrated into the existing control system of a WTS with only one extra loop proportional to the grid frequency.

The wind power penetration level in this paper is defined as the total installed capacity of WTSs over the total installed capacity of all the generators in the system. The ROCOF in this paper is obtained as the rate of change of frequency measured over a rolling window of 250 ms [16]. In this paper only under-frequency event is considered, considering that under-frequency problem is harder to be handled by WTSs compared with an over-frequency problem due to the fact that extra energy is required to be injected to the power system. It should be pointed out that our proposed method is a non-communication based decentralized design and the frequency to be regulated is the output of the existing PLL in the control system of a WTS where there are no remote signals and hence communication links with other wind turbines or the power grid are not needed. However, it should be mentioned that communication-based frequency regulation is also a potential option though it is not the scope of this paper. Under such control framework, the distributed cooperative control as proposed in [17]–[19] are promising, where only neighboring generation plants are communicated with each other, with detailed considerations of practical communication delay and uncertain communication links.

The paper is organized as follows. Section II introduces the conventional and proposed fast frequency support control. Section III presents simulation results. Section IV concludes the paper.

II. PROPOSED SCHEME FOR FAST FREQUENCY SUPPORT

A. MODELLING AND CONTROL OF DFIG-BASED AND PMSG-BASED WTS

Fig. 1 shows the configuration and control structure of doubly fed induction generator (DFIG)- and permanent magnetic synchronous generator (PMSG)-based WTSs. The detailed control systems are described in [20] and [21]. In Fig. 1, the wind turbine captures power from wind [22]. The pitch-angle controller is used to limit the rotor speed when wind speed is higher than the rated value. The rotor-side converter (RSC) controller performs MPPT control, and the grid-side converter (GSC) controller stabilizes the DC-link voltage. In the inner current controller, current vector control with feedforward decoupling and compensation terms, and Park and Park inverse transformations are implemented.

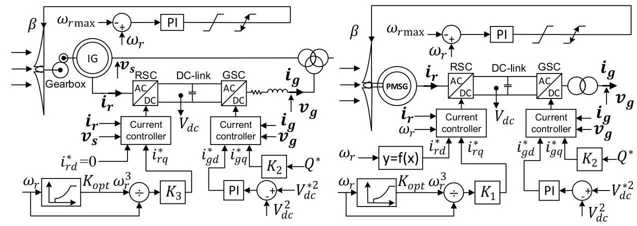

(a) DFIG-based WTS (b) PMSG-based WTS

$\boldsymbol{i_r}, \boldsymbol{v_r}, \boldsymbol{i_g}, \boldsymbol{v_g}$: three-phase current and voltage measured at rotor side and grid side, i_{rd}^*, i_{rq}^*, i_{gd}^*, i_{gq}^*: current references, V_{dc}^*, V_{dc}: DC-link voltage reference and measured value, β: pitch angle, K_1, K_2, K_3: constants, Q^*: reactive power reference.

FIGURE 1. Control structure of DFIG and PMSG-based WTSs used in this paper.

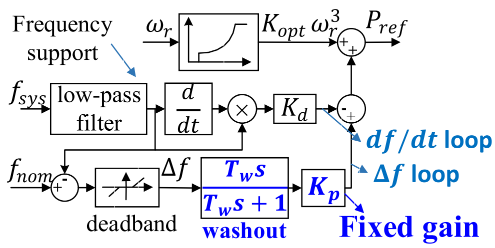

FIGURE 2. Control structure of the conventional fast frequency support scheme.

B. CONVENTIONAL FAST FREQUENCY SUPPORT SCHEME [23]

Fig. 2 shows the conventional frequency support scheme [23]. In Fig. 2, f_{sys} and f_{nom} are the measured and nominal frequency, respectively, and the low-pass filter is for the measurement delay of f_{sys} and eliminating the noise in f_{sys}. The auxiliary df/dt and Δf loops, which have fixed gains K_d and K_p, are used to improve the ROCOF and FN during a frequency event. The conventional frequency support scheme originates from the traditional SG-based system by mimicking the inertial and primary response of SGs. However, due to the fact that WTSs cannot provide persistent power like SGs since WTSs input power depends on wind, a washout component is used to eliminate the DC element of Δf in order to recover the rotor speed to the MPPT operating point after a short-term frequency support, i.e. df/dt and Δf loops become zero.

However, there are two disadvantages in the conventional frequency support scheme:

1) The first one is that the washout component gradually reduces Δf to recover the rotor speed to the MPPT operating point during the primary frequency control period. Since outputs from WTSs need to be reduced for rotor speed recovery, a delayed (even bigger) FSD will occur if Δf is reduced too fast before the SGs pick up the excess demand and restore the frequency in the system. To avoid FSD, the time constant of the

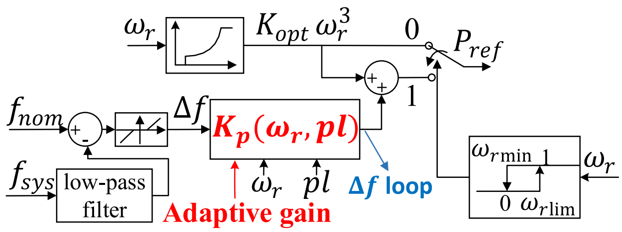

FIGURE 3. Control structure of the proposed fast frequency support scheme.

washout component together with the gains have to be carefully designed to limit the kinetic energy released for frequency support and ensure that the recovery time is sufficiently long.

2) The second disadvantage is that the additional loops for frequency support have fixed gains, which is not suitable for different wind speeds and wind power penetration levels and cannot ensure stability of WTSs. This is because the releasable kinetic energy of a WTS under different wind speeds and the required short-term frequency support under different wind power penetration levels are different.

C. PROPOSED ADAPTIVE GAIN-BASED FAST FREQUENCY SUPPORT SCHEME WITH NO ROTOR SPEED RECOVERY

The proposed adaptive gain-based fast frequency support scheme aims to:

(i) eliminate FSD;

(ii) arrest FN to be close to the settling frequency;

(iii) ensure superb FN improvements under medium and high wind speeds and different wind power penetration levels;

(iv) ensure WTSs stability under all wind speeds and system operating conditions.

Fig. 3 shows the control structure of the proposed scheme. The hysteresis comparator is to ensure that a WTS has the frequency support function only when its rotor speed is above $\omega_{r\lim}$, which is denoted as the speed limit. It can be obtained through simulation studies so that the WTS under $\omega_{r\lim}$ will have sufficient kinetic energy for providing frequency support.

1) NO ROTOR SPEED RECOVERY DURING THE PRIMARY FREQUENCY CONTROL

In the proposed frequency support scheme shown in Fig. 3, no washout component is used, so Δf loop will not become zero, and the rotor speed of a WTS will not recover to the optimal point during the primary frequency control. Thus, no extra energy will be extracted from the grid for rotor speed recovery and there will be no FSD. As a result, the releasable kinetic energy can be much larger to improve FN to be close to the settling frequency. Furthermore, when the frequency is gradually regulated to the nominal value during the secondary frequency control, Δf loop will gradually reduce to zero, leading to an automatic recovery of rotor speed. Therefore, no complicated rotor speed recovery curve needs to be designed. It should be mentioned that it is impossible to control FN to be close to the settling frequency if the rotor speed is designed to recover to the optimal operating point. This is because the recovery inevitably requires extra energy from the grid. In the proposed scheme, FN can be raised close to the settling frequency because the recovery is handled by the secondary frequency control, during which the frequency is picked up to the nominal value by injecting extra energy from other devices.

Apart from the advantage of no rotor speed recovery, the power reference $K_{opt}\omega_r^3$ of MPPT control remains in the proposed controller. The extra Δf loop being used to realize the frequency support should also be highlighted, although they are not new. In [8], [9], [11], the over-production of power for frequency support does not use frequency as a feedback input, which is hard to suit for different frequency events and system responses. Moreover, it becomes more difficult to decide the beginning and rate of decrease of over-production in order to reduce SFD. In [8]–[12], during the over-production and rotor speed recovery, the MPPT control power reference $K_{opt}\omega_r^3$ is fixed at the value of pre-disturbance by assuming a constant wind speed. This is inadequate as it is known that the wind speed is rarely constant due to wind turbulence [24], [25]. Instead, the two components of $K_{opt}\omega_r^3$ and Δf are adopted in the proposed frequency support scheme. The reasons are: (i) $K_{opt}\omega_r^3$ will gradually decrease with the reduction of ω_r during the short-term frequency support, making a WTS automatically stable at a power output lower than the one with MPPT control once the electrical output power is equal to the mechanical input power. This is because ω_r reflects the energy level of a WTS and will automatically reduce during the frequency support to force the output electrical power to follow the captured mechanical power. As shown in Fig. 4, during the power support the power reference $K_{opt}\omega_r^3$ decreases with the decrease of ω_r from point A to point C. This makes the WTS electrical power output automatically decrease along curve DB and stabilized at point B which is lower than point A of MPPT control. From the proposed control algorithm shown in Fig. 3 it is known that BC equals to $K_p\Delta f$. (ii) $K_{opt}\omega_r^3$ makes a WTS automatically and smoothly switch between the MPPT operation and frequency support operation. (iii) $K_{opt}\omega_r^3$ inherits the benefits of MPPT control which can adapt the change of wind speed during the primary frequency control. (iv) Using f as a feedback input can simplify the design of frequency support and can automatically adapt to different frequency events and system conditions.

From the analysis above it can also be seen that holding FN to be close to the settling frequency makes the output power of a WTS decline smoothly and stabilized at a point where the electrical power equals to the captured mechanical power with little oscillations, unlike the oscillating characteristics of SGs. This shows another benefit of the proposed strategy of holding the FN close to the settling frequency by providing fast frequency support through making full use of the large kinetic energy stored in WTSs.

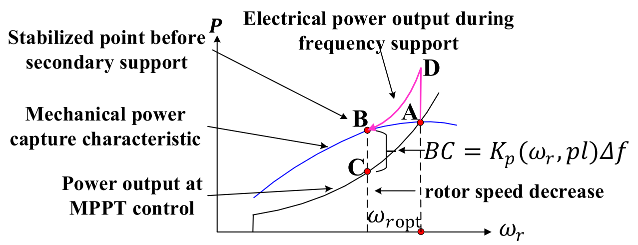

FIGURE 4. The output electrical power and captured mechanical power during the proposed fast frequency support.

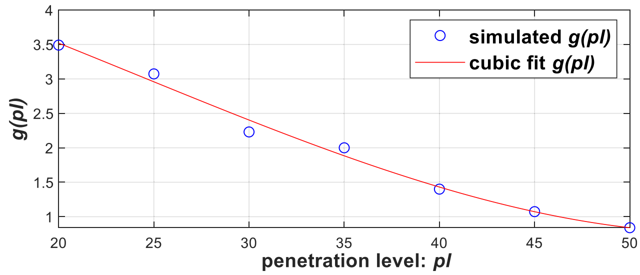

FIGURE 5. The expression of $g(pl)$ by using cubic fitting function based on the simulated data of the test system in Section III.

The side effect of the proposed scheme is that the settling frequency will be slightly lower than that of the scheme where the rotor speed is recovered to the MPPT operating point due to the loss of wind power capture. As shown in Fig. 4 and the simulation results in Section III, the wind power capture loss is minimal, which is less than 1% of the maximum wind power capture, and the settling frequency is only slightly lower (within 0.03 Hz when $pl \leq 70\%$) than that when WTSs is operated at MPPT control.

2) ADAPTIVE GAIN

The third and fourth goals mentioned above can be achieved by the adaptive gain $K_p(\omega_r, pl)$, which is given by

$$K_p(\omega_r, pl) = g(pl) * k(\omega_r) \tag{1}$$

where pl represents the wind power penetration level.

In (1), the adaptive gain $g(pl)$ is used to adapt to different wind power penetration levels by considering the rated wind speed, and $k(\omega_r)$ is used for achieving the consistent FN improvements under different wind speeds at each penetration level. In practice, the expression of $g(pl)$ can be obtained by utilizing linear or nonlinear fitting functions based on discrete values of $g(pl)$ obtained from simulations. In each simulation, the wind penetration level is fixed and the worst frequency event is simulated under the rated wind speed. Then each discrete value of $g(pl)$ is obtained so that FN is raised to be close to the settling frequency.

Fig. 5 shows the obtained $g(pl)$ by using cubic polynomial fitting function based on the simulated data using the test system described in Section III. From Fig. 5 it can be seen that $g(pl)$ decreases with increasing pl. This is because WTSs are used to quickly compensate the slow power output from SGs to arrest the frequency during the first few seconds of a frequency event, thus at a higher pl the total number of WTSs will be larger and the required fast power output increase from each WTS will be less.

In (1), when $g(pl)$ is used for different pl at the rated wind speed to regulate FN to be close to the settling frequency, $k(\omega_r)$ is used for different wind speeds under each penetration level to achieve the similar FN improvement and ensure stable operation of WTSs. It is given by:

$$k(\omega_r) = \sqrt{\omega_r - \omega_{r\min}} \tag{2}$$

where $\omega_{r\min}$ is the minimum rotor speed.

From (2) it can be seen that when the wind speed is higher than the rated speed and then ω_r is controlled at $\omega_{r\max}$ by the pitch angle control, $k(\omega_r)$ is fixed at $\sqrt{\omega_{r\max} - \omega_{r\min}}$. When the wind speed is lower than the rated speed, the WTS is under MPPT operation so the initial $k(\omega_r)$ is equal to $\sqrt{\omega_{ropt} - \omega_{r\min}}$, where ω_{ropt} relies on the input wind speed. As a result, when the wind speed is lower than the rated speed the initial $k(\omega_r)$ is different under different wind speeds and it becomes larger at a higher wind speed. This is understandable because:

1) Under a higher wind speed, the ratio of the wind power generation over the total power generation of a system is higher, causing a higher ROCOF and FN under a same frequency event. Thus, at a higher wind speed more kinetic energy is required to be released, which requires a larger gain to quickly arrest FN.
2) When wind speed decreases to medium, less kinetic energy is stored in the rotor, thus a smaller gain will not cause an over-deceleration of rotor speed and a large loss of wind power capture.

Equation (2) also shows that the stability of a WTS can be ensured as explained below. (i) During the process of frequency support the gain $k(\omega_r)$ will decrease with the decrease of ω_r due to the release of kinetic energy. The decrease of $k(\omega_r)$ means a reduction of frequency support, which in turn slows down the further reduction of the rotor speed. This helps to avoid excessive reduction of the rotor speed even if a consecutive frequency event happens. This also means that the rotor speed can always be bigger than $\omega_{r\min}$ if the rotor speed prior to a frequency event is already bigger than $\omega_{r\min}$, because if ω_r decreases close to $\omega_{r\min}$, $k(\omega_r)$ will become close to zero, which stops further frequency support and thus the further decrease of the rotor speed. (ii) If the input wind speed decreases during a period of frequency support, $k(\omega_r)$ will automatically decrease since the decrease of the wind speed will lead to the decrease of the input mechanical power and then the rotor speed ω_r.

Alternatively, $k(\omega_r)$ can also be set as one of the functions of $(\omega_r - \omega_{r\min})$, $\sqrt[3]{\omega_r - \omega_{r\min}}$, $(\sqrt{\omega_r} - \sqrt{\omega_{r\min}})$, or other functions. The difference among these functions and (2) is that the ratio of frequency support capability under medium wind speeds over that under rated wind speed is different. To enable a strong frequency support at a medium wind speed

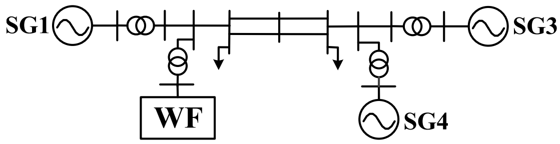

FIGURE 6. **The modified two-area system with an aggregated DFIG-based WF.**

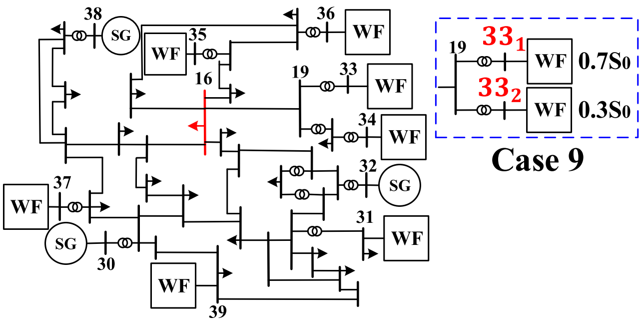

FIGURE 7. **The modified IEEE 39-bus power system with aggregated PMSG-based WFs, where S_0 means the rated capacity of each WF or SG.**

similar to that at the rated wind speed, functions with higher ratios should be chosen. In such situation, $\sqrt{\omega_r - \omega_{r\min}}$ or $\sqrt[3]{\omega_r - \omega_{r\min}}$ can be selected.

From the analysis in this subsection, it can be seen that the proposed control strategy shown in Fig. 3 can achieve its aims with simplicity, through the arrangement of the two real-time feedback signals of system frequency and WTS rotor speed which reflect the system and WTS condition, respectively.

III. CASE STUDIES

A two-area power system and a 39-bus power system, as shown in Fig. 6 and Fig. 7, are used to demonstrate the dynamic performance of the proposed fast frequency support scheme. The parameters of synchronous generators (SGs) with automatic voltage regulators (AVRs) and/or power system stabilizer (PSSs), network, and loads for the two-area and 39-bus systems are the same as that in [26] and [27], respectively. The turbine-governor model [26] used for SGs in the 39-bus system is shown in Fig. 8. The parameters of the DFIG- and PMSG-based WTSs are the same as those in [28], which is shown in Table 2 in the Appendix. The parameters of the proposed frequency control (in Fig. 3) are shown in Table 3 in the Appendix. The proposed approach in this paper is focused on the utilization of large scale wind farms to provide frequency support control to electricity transmission system operators. Therefore all the case studies have been targeting at large-scale transmission networks (Fig. 6 and Fig. 7), while both electricity distribution systems and small scale wind farms are not the focus of this paper. The system frequency used for WTSs fast frequency support is the output of the existing PLL of a WTS, and then filtered by a low-pass filter. In the rest of this Section, the frequency shown in the simulation results is the value by dividing rotor speed of a SG by 2π. The x-axis in all the following simulation

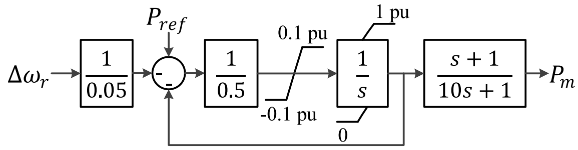

FIGURE 8. **The turbine-governor model used for SGs in the 39-bus system.**

results represent time in seconds. It should be noted that only primary frequency control is implemented in the SGs in the two systems, thus the system frequency is not expected to recover to the rated value after a frequency event. As can be seen from the closed-loop transfer function for power system frequency shown in Figure 11.25 in [26], the frequency response (and thus frequency nadir) is mainly affected by turbine-governor response of SGs, inertial time constant of SGs, power response of loads and other regulators, e.g. renewables. Thus, in this paper, the response by using the kinetic energy of WTSs on FN and frequency response are thoroughly studied in the following simulations, while the parameters of the turbine-governors, inertial time constants of SGs, and load impedance are the same as those in the original system [26], [27].

A. SIMULATIONS BASED ON THE TWO-AREA SYSTEM

Case 1-6 are simulated based on the two-area system [24], which is modified by replacing one SG with an aggregated DFIG-based WF. To consider different levels of wind power penetration, the rated capacities of SGs are modified accordingly, but all are with 0.8 p.u. active power output. For the purpose of comparison, in the following case studies, "MPPT operation" means that the WF works under MPPT operation during a frequency event and does not provide frequency support; "SG operation" means that the WF of the above system is replaced by a SG which has the same active power output as the WF and whose rated capacity is regulated to generate 0.8 p.u. active power output. Since SGs are equipped with primary frequency response, the settling frequency under "SG operation" after an under-frequency event is bigger than "MPPT operation". In order to create under-frequency events for all the following case studies, a sudden increase of 0.03 p.u. of the total load is applied.

1) BENEFIT OF NO ROTOR SPEED RECOVERY DURING PRIMARY FREQUENCY CONTROL

Case 1 is simulated to verify that a WF can arrest FN to be close to the settling frequency without FSD under the proposed scheme. To demonstrate this, the conventional frequency support scheme (shown in Fig. 2) is simulated in the same power system. In order to have a fair comparison, the df/dt loop in the conventional scheme is removed, and the gain for the Δf loop and the washout component time constant T_w are set as 0.8 and 5 s, respectively, so that the frequency under the conventional scheme can stabilize within 40 s.

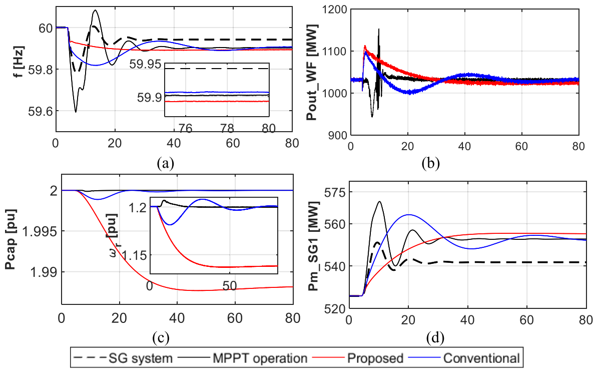

FIGURE 9. **Results for Case 1 (pl = 35%, v_w = 12m/s). (a) Grid frequency. (b) Output power of the WF. (c) Captured power of a WTS (Inside is rotor speed of a WTS). (d) Mechanical output power of SG1.**

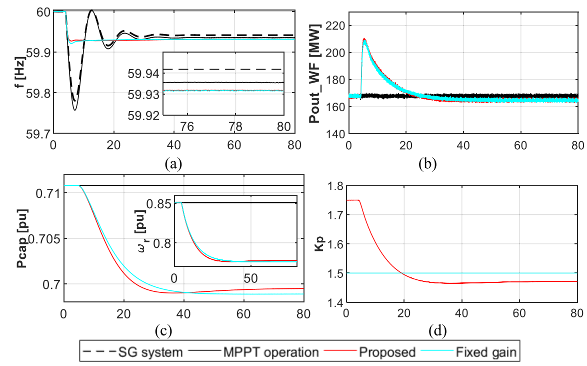

FIGURE 10. **Results for Case 2 (pl = 20%, v_w = 8.5m/s). (a) Grid frequency. (b) Output power of the WF. (c) Captured power of a WTS (Inside is rotor speed). (d) Gain of the Δf loop.**

Case 1: pl = 35%, wind speed =12 m/s.

The simulation results for Case 1 are shown in Fig. 9. Fig. 9(a) shows that with the proposed scheme, the FN is raised to be close to the settling frequency, and is increased by 0.29 Hz compared with that under the MPPT operation, while with the conventional scheme the FN is only increased by 0.22 Hz, in other words, the increase in FN using the proposed frequency support scheme with respect to the MPPT operation is about (0.29 - 0.22)/0.22 = 32% higher than that using the conventional frequency support scheme, although the maximum over-production of both schemes are almost the same in the initial support stage, as can be seen in Fig. 9(b). This is because, as shown in Fig. 9(b), under the conventional scheme the over-production only lasts for about 7 s and then quickly reduces to a much lower level before the SGs picking up the excess demand and restoring the power balance in the system. However, under the proposed scheme the over-production reduces much slower and lasts for about 22 s, leaving sufficient time for the SGs to pick up the excess demand. In the conventional frequency support scheme, the quick reduction of the over-production and the big down-production are needed to recover the rotor speed to the optimal point (Fig.9(c)), whereas in the proposed scheme no such requirement is needed. Fig. 9(a) - (b) also show that under the proposed scheme the grid frequency and output power of the WF have no oscillations, while under the conventional scheme the frequency and output power have several oscillations and take a longer time to settle.

Fig. 9(c) shows that the stabilized wind power capture under the proposed frequency support is only 0.6% lower than that under the MPPT operation. This makes settling frequency under the proposed scheme only 0.01 Hz lower than that under the MPPT operation, as can be seen from Fig. 9(a). Fig. 9(d) shows that under the proposed scheme the mechanical power from SG1 increases at a slower speed without oscillations (thanks to the smooth decrease and no rebound process of the output power of WF), which means that with the proposed scheme the mechanical fatigue of the SGs can be relieved. Fig. 9(c) also shows that the rotor speed of a WTS does not oscillate (thanks to the FN is holding to be close to the settling frequency, i.e. no frequency oscillations), which means that the mechanical pressure of a WTS because of the extra frequency support can be alleviated compared with that under the conventional scheme. This is especially beneficial for offshore WTSs which have large capacities.

2) BENEFIT OF THE PROPOSED ADAPTIVE GAIN

Case 2 - Case 5 are simulated to verify that the proposed adaptive gain $K_p(\omega_r, pl)$ can automatically regulate the over-production of the WF under different wind speeds and wind power penetration levels so that FN can be arrested to be close to the settling frequency under those conditions. To demonstrate this, a frequency support scheme with fixed gain is also simulated. The fixed gain scheme is the same as the proposed scheme except that the gain is fixed at 1.5. This value is chosen to improve FN as much as possible and ensure the stability of WTSs at wind speed of 8.5 m/s and wind power penetration level of 20%.

Case 2: pl=20%, wind speed=8.5 m/s.
Case 3: pl=20%, wind speed=12 m/s.
Case 4: pl=50%, wind speed=8.5 m/s.
Case 5: pl=50%, wind speed=12 m/s.

The simulation results for Case 2, Case 3, Case 4 and Case 5 are shown in Fig. 10, Fig. 11, Fig. 12 and Fig. 13, respectively. Fig. 12 shows the system frequency of Case 4 and Case 5 with extended simulation time. There are no simulation results of MPPT operation in Fig. 13 for Case 5 and in Fig. 15 for Case 6 since at MPPT operation the system becomes unstable with the frequency event.

Fig. 10(a) (c) show that at wind speed of 8.5 m/s and penetration level of 20%, the FN exhibits similar improvement under the proposed and fixed gain frequency support schemes. At the same penetration level of 20%, Fig. 11(a) shows that at wind speed of 12 m/s, a better FN improvement under the proposed frequency support scheme is achieved since more kinetic energy is released, as can be seen from Fig. 11(b). This is because the gain under the proposed scheme is increased at higher wind speed while the gain is

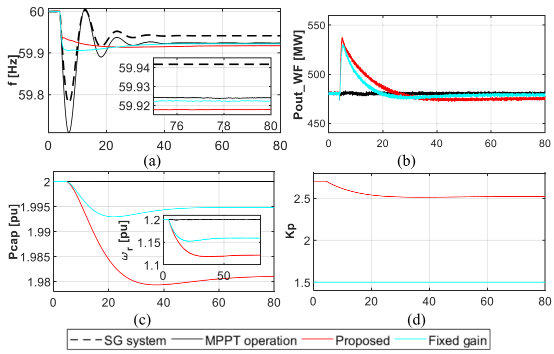

FIGURE 11. Results for Case ($pl = 20\%$, $v_W = 12m/s$). (a) Grid frequency. (b) Output power of the WF. (c) Captured power of a WTS (Inside is rotor speed). (d) Gain of the Δf loop.

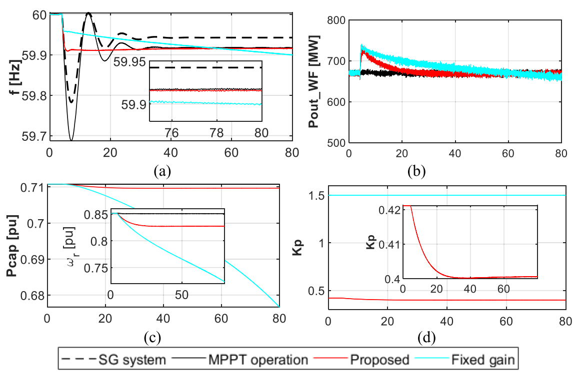

FIGURE 12. Results for Case 4 ($pl = 50\%$, $v_W = 8.5m/s$). (a) Grid frequency. (b) Output power of the WF. (c) Captured power of a WTS (Inside is rotor speed). (d) Gain of the Δf loop.

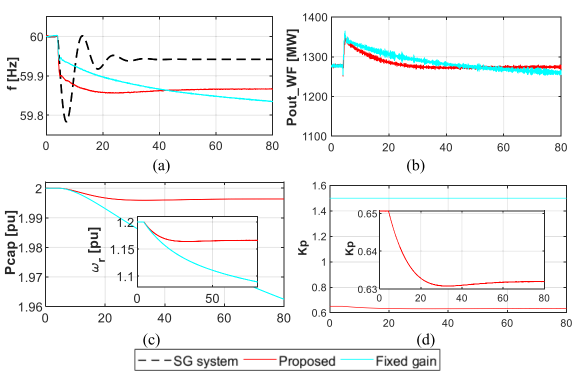

FIGURE 13. Results for Case 5 ($pl = 50\%$, $v_W = 12m/s$). (a) Grid frequency. (b) Output power of the WF. (c) Captured power of a WTS (Inside is rotor speed). (d) Gain of the Δf loop.

maintained the same under the fixed gain scheme, which can be seen by comparing Fig. 10(d) and Fig. 11(d).

Fig. 12 and Fig. 13 show that the fixed gain of 1.5 is no longer suitable at penetration level of 50%. The large gain causes excessive release of kinetic energy thus leading to significant loss of wind power capture and over-deceleration of the rotor speed, as can be seen from Fig. 12(b) - (c) and Fig. 13(b) -(c). Fig. 12(c) and Fig. 13(c) show that the rotor speed and wind power capture keep decreasing, leading to the decrease of frequency (Fig. 12(a)). The extended simulation

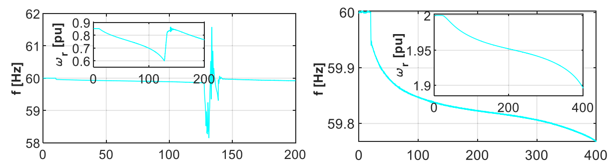

(a) For Case 4 ($pl = 50\%$ $V_{wind} = 8\,5\ m/s$). (b) For Case 5 ($pl = 50\%$ $V_{wind} = 12\ m/s$)

FIGURE 14. Grid frequency (Inside is rotor speed) under the fixed gain frequency support scheme with extended simulation time.

results in Fig. 14(a) show that at 125 s the rotor speed is reduced to the cut-in value 0.6 p.u., which forces the WTS to be switched to MPPT control and thus causes frequency oscillations. The simulation results in Fig. 14(b) show that the frequency is already reduced to an unbearable value at 400 s when no remedy is done. It should be noted that the cut-in wind speed is 6 m/s so 8.5 m/s wind speed is not low.

However, under the proposed frequency support scheme, the gain $K_p(\omega_r, pl)$ is reduced by the decrease of $g(pl)$ at higher penetration level, which can be seen by comparing Fig. 12(d) and Fig. 13(d) with Fig. 10(d) and Fig. 11(d), respectively. Comparing Fig. 10(d) with Fig. 11(d), and Fig. 12(d) with Fig. 13(d), it can be seen that at the same penetration level under different wind speeds the gain $K_p(\omega_r, pl)$ is also different. In summary, Fig. 10(a), Fig. 11(a), Fig. 12(a) and Fig. 13(a) show that the dynamic gain $K_p(\omega_r, pl)$ ensures that the FN is always close to the settling frequency under different penetration levels and wind speeds. Comparing Fig. 12(c) and Fig. 13(c) with Fig. 10(c) and Fig. 11(c), respectively, it can be seen that at a higher penetration level, the loss of wind power capture becomes less when achieving the aim of arresting FN to be close to the settling frequency. This is because the required power support from each WTS is less at a higher wind power penetration level. Fig. 12(c) and Fig. 13(c) show that the loss of wind power capture is minimal, i.e. less than 0.2%. From the above analysis, it can be seen that it is important that the gain of the Δf loop for frequency support should be properly designed to cater for different wind speeds and wind power penetration levels.

3) COMPARISON OF PROPOSED DYNAMIC GAIN WITH GAIN USED IN [13] UNDER A FIXED PENETRATION LEVEL

This section is to validate that under the proposed scheme FN can be raised to be close to the settling frequency at not only high wind speed but also medium wind speed. To demonstrate this, the kinetic energy-based gain used in [13] is used as comparison, where the gain is already reduced significantly when the wind speed is still sufficiently high. The kinetic energy-based gain in [13] is expressed as $AG_i(\omega_r) = C(\omega_r^2 - \omega_{r\min}^2)$. To make a fair comparison, the constant C for Cases 6-7 is chosen to make the frequency support gain $AG_i(\omega_r)$ equal to the proposed frequency support gain $K_p(\omega_r, pl)$ at wind speed of 12 m/s and wind power penetration level of 30%. It should be noted that in [13] the aims of the gain design are to improve FN and ensure stability of WTSs under variable wind speeds,

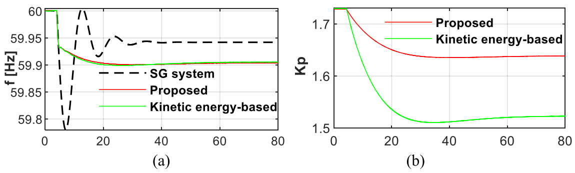

FIGURE 15. **Results for Case 6 (pl = 30%, v_w = 12m/s). (a) Grid frequency. (b) Gain of the Δf loop.**

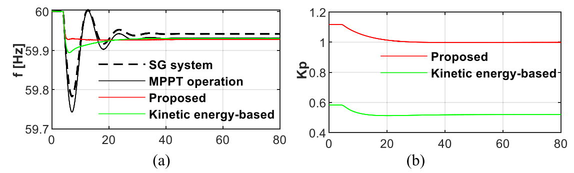

FIGURE 16. **Results for Case 7 (pl = 30%, v_w = 8.5m/s). (a) Grid frequency. (b) Gain of the Δf loop.**

while penetration level is not considered, FN is not proposed to be raised to be close to the settling frequency, and the issue of rotor recovery strategy is not mentioned.

Case 6: pl=30%, wind speed=12 m/s.

Case 7: pl=30%, wind speed=8.5 m/s.

The simulation results for Case 6 and Case 7 are shown in Fig. 15 and Fig. 16, respectively. Fig. 15 shows that very similar FN improvement is achieved by both adaptive gains. Fig. 16 shows that much better FN improvement is achieved with the proposed adaptive gain. This is because the kinetic energy-based gain at wind speed of 8.5 m/s is already reduced to be much smaller than that at the rated wind speed of 12 m/s. Hence, the stored kinetic energy cannot be fully released when the wind speed is not sufficiently low. Fig. 16(a) shows the difference of FN improvement between the two methods at wind power penetration of 30%. It can be expected that the difference will become bigger as wind power penetration level is further increased.

4) EXTRA CONVERTER CAPACITY REQUIREMENT IN A WTS

In order to provide the frequency support, additional current rating is required for the converters of a DFIG-based WTS in comparison to the conventional MPPT control strategy. In Table 1, P_{wf} is the output power of the WF under MPPT control, $P_{out-peak}$ is the peak power output of the WF during frequency support, and $\Delta P_{wts} = \frac{P_{out-peak} - P_{wf}}{Num.}$ is the extra power output of a single DFIG-based WTS compared to that under MPPT control. The additional required current rating under different penetration levels is calculated as $\Delta I\% = \frac{0.3*\Delta P_{wts}}{0.3*ratedcapacityofaWTS}$ considering that the capacity of converters in a DFIG-based WTS is usually 0.25∼0.3 times of the rated capacity of a WTS (2.2 MW in this paper). The rated wind speed of 12 m/s is chosen to calculate the required additional current rating of converters. This is because under 12 m/s, the extra power output of a WTS is the largest and during that time there is no capacity left of converters for the extra power output.

TABLE 1. **Simulation results for extra current rating calculations.**

pl	v_w (m/s)	$Num.$ WTSs	P_{wf} (MW)	$P_{out-peak}$ (MW)	ΔP_{wts} (MW)	$\Delta I\%$
20%	12	247	480	538	0.2348	10.67%
30%	12	423	822	894	0.1702	7.74%
35%	12	531	1032	1100	0.1281	5.82%
50%	12	657	1277	1345	0.1035	4.7%

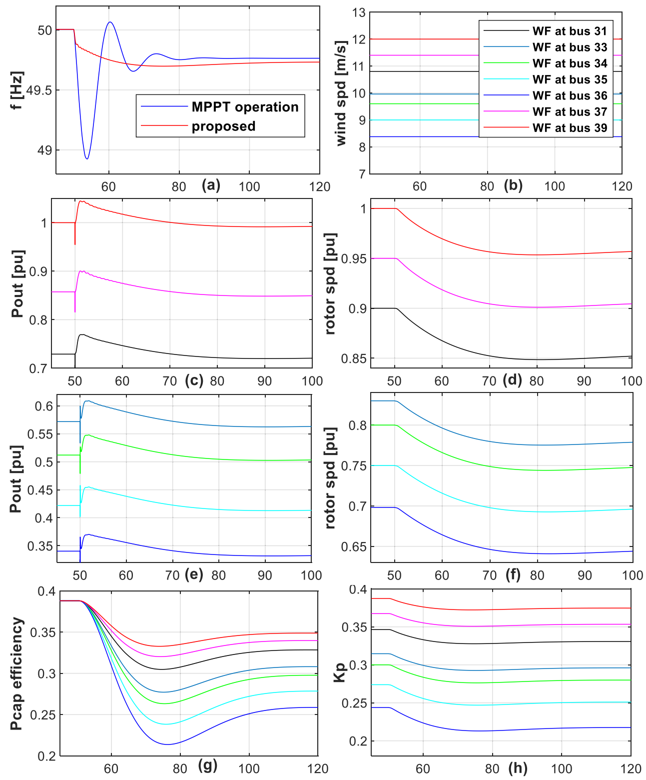

FIGURE 17. **System frequency and responses of the seven WFs under the proposed control for Case 8 (pl = 70%, different constant wind speeds for WFs).**

B. SIMULATIONS BASED ON THE 39-BUS SYSTEM

Cases 8-9 are simulated based on the 39-bus system [27]. As shown in Fig. 10 seven SGs are replaced by PMSG-based WFs (i.e. wind power penetration level is 70%). In Case 9, the WF connected to bus 33 is split into two WFs (see Fig. 7), where the WF connected to bus 33_2 is applied with varying wind speed obtained from [30]. In order to create under-frequency events, a sudden increase of 500 MW load is applied at bus 16 at 50 s for Case 8, and at 120 s for Case 9.

Case 8: pl=70%, different constant wind speeds for WFs.

The simulation results for Case 8 under the MPPT and proposed control schemes are shown in Fig. 17 and Fig. 18. From Fig. 17(a) it can be seen that with the proposed scheme the FN is raised to be close to the settling frequency without FSD, and increased by 0.77 Hz compared with that under MPPT operation. Moreover, under the proposed scheme the FN is postponed by 21 s, in other words the ROCOF is much reduced. Fig. 17(a) also shows that the settling frequency under the proposed control is 0.03 Hz less than that under MPPT operation, which is small even under such high pl

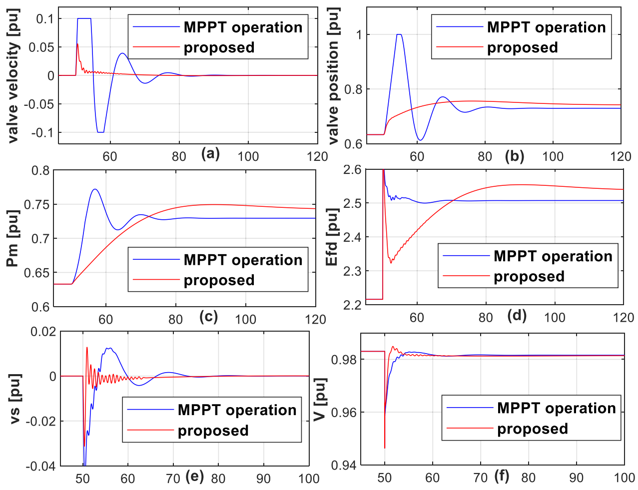

FIGURE 18. **Responses of turbine-governor and excitation system of the SG at bus 32 with the MPPT and proposed controls under Case 8 (*pl* = 70%, different constant wind speeds for WFs).**

of 70%. On one hand, this does not pose challenges to network operations considering that a secondary frequency response usually starts around 30 s after a frequency event (will probably start earlier in future) to recover the frequency. On the other hand, the greatly raised FN makes the proposed scheme highly desirable. From Fig. 17(a) it can also be seen that the frequency under the proposed scheme is smoother without overshoots, thanks to the fast frequency response of the WFs.

Fig. 17(b) shows the wind speeds for the 7 WFs ranging from 8 m/s to 12 m/s (from middle to high). Fig. 17(c)(e) shows that the power supports last around 15 s $\sim$ 20 s, and with a higher wind speed, the power support is stronger, due to the fact that a higher rotor speed leads to a larger gain $K_p(\omega_r, pl)$, as can be seen from Fig. 17(d)(f)(h). Fig. 17(d)(f)(h) also show that with decreasing rotor speeds, the proposed dynamic gains $K_p(\omega_r, pl)$ are decreasing to protect WTSs from over-deceleration. From Fig. 17(g) it is seen that the maximum loss of wind power capture is less than 1%.

With the proposed fast frequency support by WFs, the turbine-governor responses of the SG are slowed down with no oscillations and the peak values of the turbine valve velocity and position and output mechanical power become much smaller (thus the mechanical pressure is reduced), as seen from Fig. 18(a)-(c); The output of the AVR is much slowed down (the initial peak value in Fig. 18(d) is due to the use of frequency deadband in the proposed fast frequency support) as seen from Fig. 18(d); The output of the PSS is reduced due to the fact that the deviation of rotor speed of the SG is used as the PSS input, as seen from Fig. 18(e); The terminal voltage of the SG recovers quicker, as seen from Fig. 18(f). The much delayed and smaller peak responses shown in Fig. 18(a)-(e) demonstrate the benefits of using the proposed fast frequency support scheme, which gains time and reduces the required capacity for future frequency regulation units.

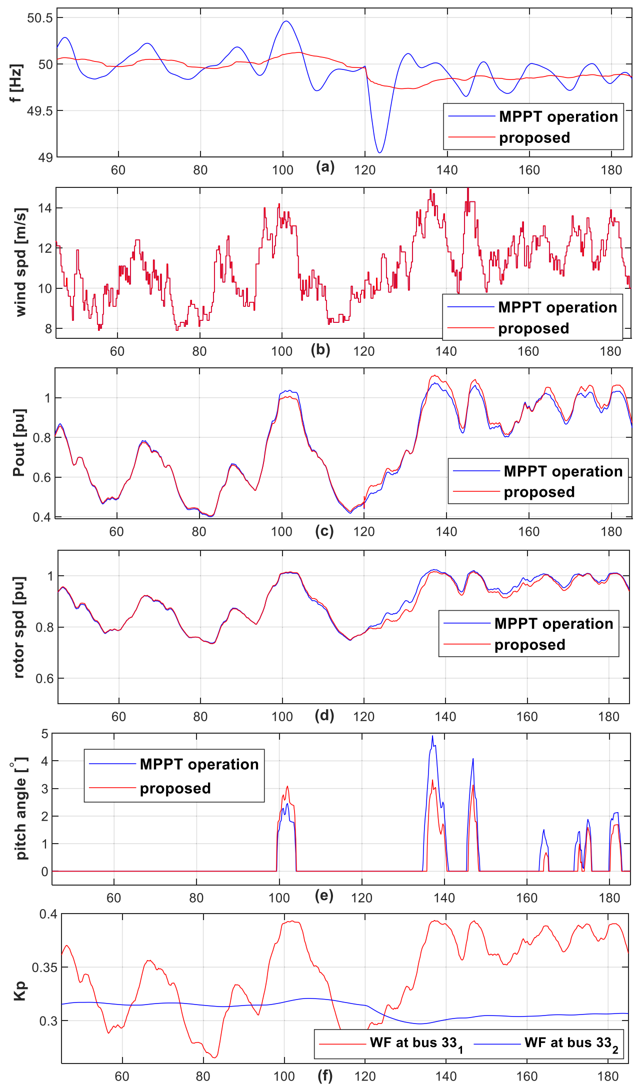

FIGURE 19. **System frequency, responses of WF at bus 33_2, and K_p of WF at bus 33_1 under Case 9 (*pl* = 70%, WF at bus 33_2 with varying wind speed).**

Case 9: pl=70%, WF at bus 33_2 with varying wind speed, the same constant wind speeds for other WFs as in Case 8.

Simulation results for Case 9 under the MPPT and proposed control schemes are shown in Fig. 19. Fig. 19(a) shows that under the proposed control, the frequency is much smoother than that under the MPPT operation. It means the wind power output can be smoothed with the proposed control method. Moreover, from Fig. 19(c)(d) it is seen that before 120 s, the output power and rotor speed under the MPPT and proposed control are overlapped, which means that the proposed scheme has minimal impact on the maximum wind power capture during normal operation. After 120 s, it can be seen from Fig. 19(a) that with the proposed control the FN is greatly raised and exhibits the same trend of being close to the settling frequency as that in Fig. 18(a). After 120 s, from Fig. 19(c)(d) it is seen that except the

TABLE 2. Parameters of DFIG- and PMSG-based WTSs.

DFIG-base WTS	Value	PMSG-base WTS	Value
Rated capacity of the turbine/DFIG	2.0 MVA/ 2.2 MVA	Rated capacity	2.0 MVA
Rated stator voltage	0.69 kV	Rated stator voltage	4 kV
Rated frequency	50 Hz	Rated frequency	3.77 Hz
Stator/rotor resistance	0.00462 p.u./ 0.006 p.u.	Pole pair	11
		Stator resistance	0.01 p.u.
Stator/rotor leakage inductance	0.102 p.u./ 0.08596 p.u.	Stator leakage inductance	0.1 p.u.
Mutual inductance	4.348 p.u.	D-/Q-axis unsaturated magnet. Inductance	0.65 p.u. /1.0 p.u.
Wind turbine/DFIG inertia constant	4.3 s/0.75 s	Magnetic strength	1.3 p.u.
		PMSG inertia constant	5.05 s

captured wind power = $0.5\rho\pi R^2 v_w^3 C_\rho(\lambda,\beta) = K v_w^3 C_\rho(v_w,\omega_r,\beta)$, where K=0.0012, v_w is in m/s, ω_r is in p.u., R=81m, and $C_\rho\sim\lambda$ curve is adopted from [22]. Cut-in and rated v_w are 6 m/s and 12 m/s. The related $\omega_{r\min}$ and $\omega_{r\max}$ for DFIG are 0.6 p.u. and 1.2 p.u. for PMSG are 0.5 p.u. and 1 p.u.

first 10 s power support of the proposed control, during 135 s $\sim$ 185 s the output power is continuously larger in the first 20 s than that under the MPPT operation. This extra power comes from the wind, as is seen from Fig. 19(e) that the pitch angle becomes smaller under the proposed control. This exhibits another benefit of the proposed control under wind speed higher than the rated value. Fig. 19(f) confirms that the change of the proposed dynamic gains $K_p(\omega_r, pl)$ follows that of the rotor speed.

IV. CONCLUSION

This paper has proposed a fast frequency support scheme for WTSs by making use of the stored kinetic energy to significantly raise FN to be close to the settling frequency without FSD. The key contributions of the proposed scheme are:

(a) Arresting FN: FN can be significantly raised. In other words FN is arrested and raised to a high level close to the settling frequency;

(b) Ensuring consistent superb FN improvements under different operating conditions: the proposed adaptive gain is a function of the real-time rotor speed and wind power penetration level. This ensures consistent superb FN improvements under both medium and high wind speeds and different penetration levels;

(c) Avoiding FSD by a new speed recovery strategy: the rotor speed of a WTS is not required to recover to the MPPT operating point during the period of primary frequency control. In this way, the released kinetic energy can be large and no FSD will occur, because no extra energy is required to be extracted from the grid to recover the rotor speed.

The three unique contributions above have been implemented together into the proposed frequency support scheme so that FN can be significantly raised and arrested. From the test case, the increase in FN using the proposed frequency support scheme with respect to the MPPT operation is 32% higher than that using the conventional frequency support scheme. Under both medium and high wind speeds and different penetration levels, the consistent superb frequency support performance and the stability of WTSs have been verified by comparisons of simulation results using the two-area power system with a DFIG-based WF and the 39-bus power system with PMSG-based WFs; The recent power cut incident in the UK on 9th August 2019, which resulted in tens millions of economic loss, indicated that the proposed frequency control to raise FN and eliminate FSD is highly desirable for the security and reliability of power grids with high penetration of wind energy.

TABLE 3. Parameters of proposed fast frequency support.

Symbol	Value	Symbol	Value
loss-pass filter time constant	0.02 s	dead-band for Δf	$\pm$0.02 Hz
$\omega_{r\min}$ and $\omega_{r\lim}$ for DFIG/PMSG		0.6p.u./0.5 p.u., and 0.7 p.u./0.6 p.u	
$g(pl)$ in (4) for pl=20%, 30%, 35%, 50% and 70% is 3.49, 2.23, 2.0, 0.84, 0.6.			

APPENDIX

See Tables 2 and 3.

REFERENCES

[1] (2019). *Technical Report on the Events of 9 Aug. 2019, National Grid Electricity System Operator*. [Online]. Available: https://www.ofgem.gov.uk/system/files/docs/2019/09/eso_technical_report_-_final.pdf

[2] M. Tsili and S. Papathanassiou, "A review of grid code technical requirements for wind farms," *IET Renew. Power Generat.*, vol. 3, no. 3, pp. 308–332, Sep. 2009.

[3] R. G. de Almeida and J. A. Pecas Lopes, "Participation of doubly fed induction wind generators in system frequency regulation," *IEEE Trans. Power Syst.*, vol. 22, no. 3, pp. 944–950, Aug. 2007.

[4] I. D. Margaris, S. A. Papathanassiou, N. D. Hatziargyriou, A. D. Hansen, and P. Sorensen, "Frequency control in autonomous power systems with high wind power penetration," *IEEE Trans. Sustain. Energy*, vol. 3, no. 2, pp. 189–199, Apr. 2012.

[5] F. Díaz-González, M. Hau, A. Sumper, and O. Gomis-Bellmunt, "Participation of wind power plants in system frequency control: Review of grid code requirements and control methods," *Renew. Sustain. Energy Rev.*, vol. 34, pp. 551–564, Jun. 2014.

[6] G. Ramtharan, J. B. Ekanayake, and N. Jenkins, "Frequency support from doubly fed induction generator wind turbines," *IET Renew. Power Gener.*, vol. 1, no. 1, pp. 3–9, Mar. 2007, doi: 10.1049/iet-rpg:20060019.

[7] J. Morren, S. W. H. de Haan, W. L. Kling, and J. A. Ferreira, "Wind turbines emulating inertia and supporting primary frequency control," *IEEE Trans. Power Syst.*, vol. 21, no. 1, pp. 433–434, Feb. 2006.

[8] P.-K. Keung, P. Li, H. Banakar, and B. Teck Ooi, "Kinetic energy of wind-turbine generators for system frequency support," *IEEE Trans. Power Syst.*, vol. 24, no. 1, pp. 279–287, Feb. 2009.

[9] N. R. Ullah, T. Thiringer, and D. Karlsson, "Temporary primary frequency control support by variable speed wind turbines—Potential and applications," *IEEE Trans. Power Syst.*, vol. 23, no. 2, pp. 601–612, May 2008.

[10] K. Liu, Y. Qu, H.-M. Kim, and H. Song, "Avoiding frequency second dip in power unreserved control during wind power rotational speed recovery," *IEEE Trans. Power Syst.*, vol. 33, no. 3, pp. 3097–3106, May 2018.

[11] D. Yang *et al.*, "Temporary frequency support of a DFIG for high wind power penetration," *IEEE Trans. Power Syst.*, vol. 33, no. 3, pp. 3428–3437, May 2018.

[12] M. Garmroodi, G. Verbic, and D. J. Hill, "Frequency support from wind turbine generators with a time-variable droop characteristic," *IEEE Trans. Sustain. Energy*, vol. 9, no. 2, pp. 676–684, Apr. 2018.

[13] J. Lee, G. Jang, E. Muljadi, F. Blaabjerg, Z. Chen, and Y. Cheol Kang, "Stable short-term frequency support using adaptive gains for a DFIG-based wind power plant," *IEEE Trans. Energy Convers.*, vol. 31, no. 3, pp. 1068–1079, Sep. 2016.

[14] Y.-K. Wu, W.-H. Yang, Y.-L. Hu, and P. Q. Dzung, "Frequency regulation at a wind farm using time-varying inertia and droop controls," *IEEE Trans. Ind. Appl.*, vol. 55, no. 1, pp. 213–224, Jan. 2019.
[15] M. Hwang, E. Muljadi, G. Jang, and Y. C. Kang, "Disturbance-adaptive short-term frequency support of a DFIG associated with the variable gain based on the ROCOF and rotor speed," *IEEE Trans. Power Syst.*, vol. 32, no. 3, pp. 1873–1881, May 2017.
[16] (2017). *International review of frequency control adaptation, Australia Energy Market Operator*. Melbourne, VIC, Australia. [Online]. Available: http://www.aemo.com.au
[17] J. Lai and X. Lu, "Nonlinear mean-square power sharing control for AC microgrids under distributed event detection," *IEEE Trans. Ind. Informat.*, early access, Jan. 27, 2020, doi: 10.1109/TII.2020.2969458.
[18] J. Lai, "Distributed voltage regulation for cyber-physical microgrids with coupling delays and slow switching topologies," *IEEE Trans. Syst., Man, Cybern., Syst.*, vol. 50, no. 1, pp. 100–110, Jan. 2020.
[19] J. Lai, X. Lu, and X. Yu, "Stochastic distributed frequency and load sharing control for microgrids with communication delays," *IEEE Syst. J.*, vol. 13, no. 4, pp. 4269–4280, Dec. 2019.
[20] R. Pena *et al.*, "Doubly fed induction generator using back-to-back PWM converters and its application to variable-speed wind-energy generation," *IEE Proc.-Electr. Power Appl.*, vol. 143, no. 3, pp. 231–241, 1996.
[21] M. Chinchilla, S. Arnaltes, and J. C. Burgos, "Control of permanent-magnet generators applied to variable-speed wind-energy systems connected to the grid," *IEEE Trans. Energy Convers.*, vol. 21, no. 1, pp. 130–135, Mar. 2006.
[22] D. Woodford, "Determination of main parameters for a doubly fed induction generator for a given turbine rating," Electranix Corporation, Winnipeg, MB, Canada, Tech. Rep., 2004.
[23] J. Van De Vyver, J. D. M. De Kooning, B. Meersman, L. Vandevelde, and T. L. Vandoorn, "Droop control as an alternative inertial response strategy for the synthetic inertia on wind turbines," *IEEE Trans. Power Syst.*, vol. 31, no. 2, pp. 1129–1138, Mar. 2016.
[24] F. M. Hughes, O. Anaya-Lara, G. Ramtharan, N. Jenkins, and G. Strbac, "Influence of tower shadow and wind turbulence on the performance of power system stabilizers for DFIG-based wind farms," *IEEE Trans. Energy Convers.*, vol. 23, no. 2, pp. 519–528, Jun. 2008.
[25] L. Wu and D. G. Infield, "Towards an assessment of power system frequency support from wind plant—Modeling aggregate inertial response," *IEEE Trans. Power Syst.*, vol. 28, no. 3, pp. 2283–2291, Aug. 2013.
[26] P. Kundur, *Power System Stability and Control*. New York, NY, USA: McGraw-Hill, 1994.
[27] I. Hiskens, "A study of an IEEE 10-generator, 39-bus system," IEEE PES Task Force Benchmark Syst. Stability Controls, Tech. Rep., Nov. 2013. [Online]. Available: http://www.sel.eesc.usp.br/ieee/
[28] X. Zhao, Z. Yan, and X.-P. Zhang, "A wind-wave farm system with self-energy storage and smoothed power output," *IEEE Access*, vol. 4, pp. 8634–8642, 2016.
[29] P. Giangrande *et al.*, "Considerations on the development of an electric drive for a secondary flight control electromechanical actuator," *IEEE Trans. Ind. Appl.*, vol. 55, no. 4, pp. 3544–3554, Jul. 2019.
[30] (Mar. 19, 2015). *An Aeroelastic Computer-Aided Engineering Tool for Horizontal Axis Wind Turbines*. Mar. 19, 2015. [Online]. Available:https://nwtc.nrel.gov/FAST

XIANXIAN ZHAO received the B.Eng. degree from Central South University, in 2012, and the Ph.D. degree in electronic electrical and computer engineering from the University of Birmingham, in 2018. She is currently a Senior Power System Researcher with University College Dublin. Her research interests include renewable energy conversion and energy storage systems modeling, control and applications.

YING XUE (Member, IEEE) received the B.Eng. and Ph.D. degrees in electronic electrical and computer engineering from the University of Birmingham, in 2012 and 2016, respectively. He is currently a Lecturer with the University of Birmingham. His main research area is HVDC modeling and control.

XIAO-PING ZHANG (Fellow, IEEE) is currently a Professor of electrical power systems with the University of Birmingham, U.K., the Director of Smart Grid, Birmingham Energy Institute, and the Co-Director of the Birmingham Energy Storage Center. He coauthored the first and second edition of the monograph *Flexible AC Transmission Systems: Modeling and Control*, (Springer, 2006 and 2012). He co-authored the book *Restructured Electric Power Systems: Analysis of Electricity Markets with Equilibrium Models* (IEEE Press/Wiley, 2010). He is a Fellow of IET and the Chinese Society for Electrical Engineering. He has been the Advisor to the IEEE PES U.K. and Ireland Chapter and is chairing the IEEE PES WG on Test Systems for Economic Analysis. His research interests include modeling and control of HVDC, FACTS and wind/wave generation, distributed energy systems and market operations, and power system planning, and so on.